Preprints (www.preprints.org) | NOT PEER-REVIEWED | Posted: 2 September 2020 doi:10.20944/preprints202009.0034.v1

Type of the Paper (Article)

Validation of Airborne Sensor Photogrammetric Digital Terrain and Global Digital Elevation Models around Mekelle City, Ethiopia

Hareya Birhane[1,2], Tulu B. Bedada[1,2] , Berhan Gessesse[1] and Martin Vermeer[3*]

[1]Entoto Observatory and Research Center, Ethiopian Space Science and Technology Institute, Addis Ababa, Ethiopia; hareyabirhane2006@gmail.com (H.B) ; tulubesha@yahoo.com (T.B); berhang@essti.gov.et (B.G)
[2]Geospatial Information Institute, Addis Ababa, Ethiopia
[3]Department of the Built Environment, Aalto University, Finland; martin.vermeer@aalto.fi
*Correspondence: martin.vermeer@aalto.fi (M.V); Tel.: +358 50 3574139

Abstract: The quality of photogrammetric-based derived products like orthophotos, digital terrain models (DTMs) and digital line maps as well as the global digital elevation models (DEM) are rigorously dependent on the accuracy of image orientation. This paper evaluates the vertical accuracy of aerial photogrammetric Digital Terrain Model (DTM), Shuttle Radar Topography Mission (SRTM), Advanced Spaceborne Thermal Emission and Reflectance Radiometer (ASTER) and TerraSAR-X's twin satellite of TanDEM-X (TDX) datasets against *in-situ* orthometric heights computed from ellipsoidal heights and the 2008 Earth Gravitational Model (EGM2008) derived geoid heights in Ethiopia. The quality of the four global digital elevation models was also validated against the aerial photogrammetric DTM measurements. Besides, the accuracies of the photogrammetric DTM and the four DEM products were checked for their compliance to the American Society for Photogrammetry and Remote Sensing (ASPRS) standards as well as the Ethiopian national vertical data evaluation standards. The study showed that the photogrammetric DTM is in a good agreement with the reference orthometric heights compared to SRTM, ASTER and TDX datasets. More precisely, the result has an absolute accuracy of 1.67 m at Linear Error (LE) 95% confidence level, while the absolute accuracy of SRTM3 arc seconds (SRTM3) at LE 90% (11.91 m) is better than its product specification (16 m). The absolute accuracy of SRTM1 arc second (SRTM1) (7.70 m at LE 90%) surpasses that of SRTM3, whereas the absolute accuracy of ASTER DEM is somehow below its product specification. TDX also has the same vertical accuracy (10.29 m at LE 90%) compared to its product specification (10 m). Furthermore, the vertical accuracy of the photogrammetric DTM meets the100 cm vertical accuracy of the 2015 ASPRS standard. However, it does not meet the Ethiopian national vertical data accuracy requirement standard, i.e., RMSEz of ± 0.45 m. In general, the photogrammetric DTM, SRTM1 and TDX have been proven a superior product over the SRTM3 and ASTER DEMs, and better to use these products for high-level precision and accuracy required applications.

Keywords: vertical accuracy; photogrammetric DTM; ASTER; SRTM; TanDEM-X; orthometric height; geoid height

1. Introduction

A Digital Elevation Model (DEM) represents the deviation of the Earth's topography from the global equipotential surface of the Earth that best fits to open oceans and seas, usually called the geoid. Globally, the departure of the Earth's topographic surface (land surface only) and the geoid varies between -418 m at the Dead Sea to 8,848 m at the summit of Mount Everest in Nepal, with a mean value of 840 m. A DEM is realized by measuring the height of the ground points on the actual topographic surface above or below the geoid [1-3]. With the advent of satellite technology, practical computation of the DEM involves two independent measurements: the ellipsoidal heights of the

Earth's surface with respect to the 1984 World Geodetic System (WGS84) reference ellipsoid, and the geoid heights (i.e., the vertical separation between the geoid and the WGS84 reference ellipsoid). Today, ellipsoidal heights of the Earth's surface can be determined using satellite positioning system based on navigation satellites, or from radar and stereoscopic photogrammetric remote sensing techniques integrated with the satellite's own positioning system [4, 5]. On the other hand, the geoid can be directly computed from a global gravity model, preferably refined using detailed local gravity data [6-8]. Subtracting the geoid height from the ellipsoidal height gives a vertical distance above the geoid called an orthometric height. A regular grid of orthometric heights defines a DEM. The integration of satellite remote sensing or photogrammetric techniques with navigation satellite positioning and the geoid can now provide a high resolution DEM accurate to within meter to decimeter level. High resolution DEMs are an important data source particularly in regions that are devoid of detailed topographic maps. The DEM products are important in determining geomorphological parameters (e.g. slopes, curvature, terrain roughness and aspects) that are essential for various applications in the geosciences, the environmental sciences and the spatial sciences [9]. It is also very instrumental for studying glacial geomorphology and ice-sheet reconstruction [10], volcano [11,12], landslides [13-16], seismicity [17], gravity field modelling [10,18-21], ecological modelling [22], hydrological modeling [23], watershed management [24], floodplain delineating and mapping [25], cadaster and land use planning [26], land suitability assessment for agriculture and other developmental economic infrastructures [27].

To realize these various applications, the DEMs are expected to have good accuracy and high resolution. Thus, it is necessary to evaluate the level of accuracy of the DEMs prior to their practical utilization. Based on their accuracy levels, DEMs shall be used in compliance with well-adopted mapping standards such as those of the American Society for Photogrammetry and Remote Sensing (ASPRS). In this connection, various elevation model products such as DEM derived from Interferometric Synthetic Aperture Radar (InSAR) based global elevation models (i.e., ASTER, SRTM and TDX [25, 28-34] and photogrammetric derived DEMs [11, 35] have been assessed to qualify their accuracies before using for different applications.

This study intends to contribute to a continued global scientific endeavor in assessing the quality of photogrammetric DTM and the four global DEMs. The specific aim of the paper is to evaluate the accuracy of the photogrammetric DTM and the four global DEMs (two SRTMs, ASTER and TDX) against *in-situ* orthometric heights derived from EGM2008 geoid heights and Real-Time-Kinematic based Global Navigation Satellite System (GNSS) measurements in the surroundings of Mekelle city (Northern Ethiopia). Besides, the quality of the four global digital elevation models were validated against the aerial photogrammetric DTM measurements.

2. Materials and Methods

2.1. Site Description

The study area is located in the northern part of Ethiopia, particularly in the surroundings of Mekelle and Qwiha Towns. The case study site located on the Nubian plate, approximately 780 km (ground geodesic distance) from Addis Ababa. Geographically, the study area is bounded between 13° 25' 54'' and 13° 35' 50'' north latitudes and 39° 26' 10'' and 39° 35' 6'' east longitudes (Figure 1). The landmass of the study area was formed as a part of widespread continental transgression from the east to south that took place from Triassic to Cretaceous. Generally, the study area is characterized by extremely undulating topography. The southern, south eastern, eastern and northeastern parts are defined by highly elevated mountains with extremely rugged terrain. The central low-lying, southwestern and western part of the area is almost flat, while the western part is dissected terrain. In particular, the low-lying central depression and western regions are mostly characterized by river systems that drain from SSE plateaus to NNW lowlands, and the drainage networks dominate the northwestern part of the area. More specifically, the local topography varies from 1969.4 to 2410.6 m with respect to the EGM2008 geoid model as inferred from aerial photogrammetric measurements and the gradient of the local topography ranges from 0^0 to 60% (Figure 3).

Preprints (www.preprints.org) | NOT PEER-REVIEWED | Posted: 2 September 2020 doi:10.20944/preprints202009.0034.v1

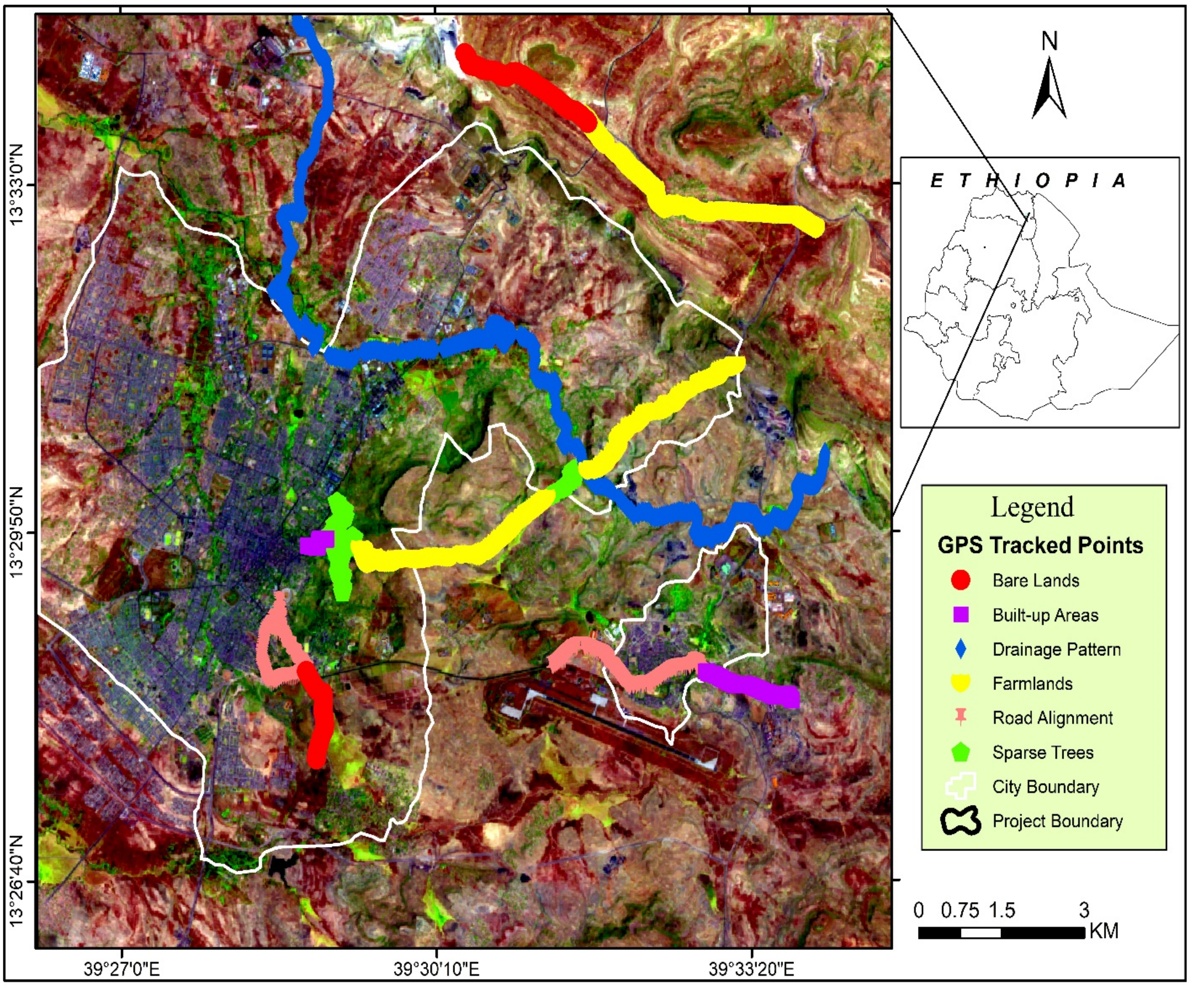

Figure 1. Location map of the study area. N.B: The background data is the false color composite of Sentinel-2A image, which was acquired in March 2020. Besides, GNSS Tracked Points were collected across six profiles. In this connection, Profile 1 represents sparse trees; Profile 2 represents Road alignment; Profile 3 represents Drainage pattern; Profile 4 represents Farmlands; Profile 5 represents Built-up areas and Profile 6 represents Bare lands.

2.2. Data Sources

2.2.1. Photogrammetric DTM

We used an aerial photogrammetric DTM that has 10 m spatial resolution. These aerial photographs were acquired by the Ethiopian Information Network Security Agency (INSA) in April 2016 (Table 1). The aerial survey was performed as part of the rural land parcel registration and good land 105 governance mission in Ethiopia. A high quality Charge Coupled Device (CCD) UltraCam Eagle camera with panchromatic, Red-Green-Blue (RGB) and Near-Infrared (NI) spectral bands was used to acquire aerial photos with Ground Sample Distance of 25 cm. The aerial photos were acquired at a nominal flight height of 2845 m above the Alexandria Mean Sea Level (AMSL) along six strips with 70% forward overlap and 30% side overlap. Aerial photos were processed with a tie to onboard aircraft navigation and attitude data as well as with reference to 4 Ground Control Points (GCPs). The GCPs (North, East and Up-coordinates of the checkpoints) were established with static GNSS observations taken for a session of 72 hours. Thus, using these aerial photographs, a very high resolution DTM was generated.

Table 1. Detailed characteristics of input dataset used for DEM products evaluation.

Dataset	Resolution	Source
Photogrammetric DTM	10 m	INSA
Shuttle Radar Topography Mission (SRTM1)	1 arc second (~30 m)	http://earthexplorer.usgs.gov
Shuttle Radar Topography Mission (SRTM3)	3 arc seconds (~90 m)	http://earthexplorer.usgs.gov
Advanced Spaceborne Thermal Emission and Reflection Radiometer (ASTER)	3 arc seconds (~30 m)	http://earthexplorer.usgs.gov
TerraSAR-X's twin satellite (TDX)	3 arc seconds (~90 m)	https://tandemx-science.dlr.de
Validation Kinematic GPS tracked data collected across different land use and terrain features	Profile Point Data	Field Measurement

2.2.2. SRTM DEMs

In this study, we also used SRTM1 and SRTM3 DEMs. The SRTMv2.1 interferometric radar payload has collected elevation data covering almost 80% of the Earth's surface between 60°N and 54°S during its 11-days mission in February 2000. This DEM is relatively low spatial resolution of 3 arc seconds (~90 m) in the rest of the world outside of USA [36]. The DEM is defined in geographic datum with a tie to WGS84 for horizontal coordinates (latitude and longitude) and the EGM1996 geoid model for elevation or orthometric height. The final product of the DEM is reported to have an absolute vertical accuracy of ± 16 m and horizontal accuracy of ± 20 m at a 90% confidence level [37]. The second DEM is SRTMv3.0 (SRTM1) obtained by filling the data gaps in the SRTM DEM with elevations acquired from the USGS's Global Muti-resolution Terrain Elevation Datasets[38].

2.2.3. ASTER DEM

The other DEM used in this study is ASTER version 2, which was released for public use in October 2011 and has a spatial resolution of 30 m. ASTER DEM is acquired from NASA Terra Satellite. With regard to accuracy, ASTER has an absolute vertical accuracy of 17 m at 95% confidence level [30]. The Terra Satellite has acquired elevation data across the landmass between 83° N and 83° S using correlation between stereo pair images acquired with 15 m spatial resolution from the visible and near infrared (VNIR) bands.

2.2.4. TanDEM-X

The German TDX 90 m DEM is the fourth global DEM product used in this study. As Wessel [39] clearly summarized, the German TDX 90 m DEM is acquired using Earth observation radar mission that consists of a SAR interferometer made up of two almost identical satellites flying in close formation for comparative analysis. The corresponding pairs of the TDX images were acquired by the twin satellites TerraSAR-X and TDX, which fly in a close helix formation with distances between 300 and 500 m of each other to generate highly accurate global DEM with complete global coverage.

2.2.5. Real time Kinematic GPS tracked Datasets

For validating the different DEMs datasets, the study also used ground truth ellipsoidal heights, which were acquired from *in-situ* based real time Kinematic GPS tracks. Based on the base map prepared using satellite imagery, six major land use/land cover classes (profiles) were identified. Accordingly, the validation points were collected along these six major different land cover classes (profiles) representing sparse trees (Profile 1); road alignment (Profile 2); drainage pattern (Profile 3); farmlands (Profile 4); built-up areas (Profile 5) and bare lands (Profile 6) (Figures 1 and 3 and Table 2).

Table 2: Operational description of land use/land cover classes considered in this study.

Profiles	classes	Descriptions	GNSS Tracked points
Profile 1	Sparse Trees	These are group of trees interspersed with bare ground and low growing ground cover.	226 points
Profile 2	Road	This refers to a long or narrow stretch with a smoothed or paved surface made for traveling by motor vehicle.	272 points
Profile 3	Drainage pattern	These features are representing small rivers and streams courses in the study area.	660 points
Profile 4	Farmland	This is a portion of land surface used for crop cultivation or capable of being cultivated.	651 points
Profile 5	Built-up area	They are features including towns, small concentrated villages roofed with corrugated iron sheet and different infrastructures.	87 points
Profile 6	Bare land	A land with limited ability to support life and it is an area of thin soil, sand, or rocks.	234 points

In this regard, Geodetic Leica receivers were used for determining position coordinates for each field point. In total, 2130 ellipsoidal heights were collected across the study area during a field campaign in April 2017 (Tables 1 and 2). In essence, RTK-based ellipsoidal heights can capture accurate topographic information (~3-5 cm) and their transformation to orthometric height maintains high accuracy up to a few centimeters (~6-10 cm), the error in the EGM2008 geoid model over Ethiopia was estimated to vary between 3 and 5 cm [6]. This makes an *in-situ* ellipsoidal heights combined with EGM2008 geoid heights a standard reference for validating the accuracy of aerial photogrammetric and satellite-based DEM products.

2.3. Methods

The geometric accuracies of aerial images were evaluated by reducing uncertainty of the exterior orientation parameters through utilizing accurate Ground Control Points (GCPs) and attitude of aircraft in a block adjustment computation of aerial triangulation. We used 4 GCPs and 5 check-points in order to ensure the production of high quality photogrammetric measurements. GCPs were established using static Differential Global Navigation Satellite Systems (DGNSS) geodetic positioning using dual-frequency receivers. In essence, 3 GCPs are suffice to perform exterior orientation that transform images (defined in a camera coordinate system) to geodetic coordinate system. In the study area, the GCPs and checkpoints were designed in such a way that they tie overlapping aerial photos to ensure the overall quality of the photogrammetric measurements. Datasets from on-board GNSS and Inertial Measurement Unit were used to establish the absolute positions and orientations of each aerial photo in a block adjustment computation. After the direct georeferencing computation, the GCPs were used to adjust the final solution, while the checkpoints were used to evaluate the accuracy of triangulated images.

Finally, the vertical accuracies of photogrammetric DTM, ASTER, TDX, SRTM1 and SRTM3 products were evaluated against the 2130 ground-based RTK GNSS measurements. Comparison was made in terms of orthometric height, as it is a physical height system that can define level surfaces on the Earth's topography. In order to perform statistical comparison between elevation models and ground truth data, RTK GNSS based ellipsoidal heights were transformed to orthometric heights defined with reference to the EGM2008 geoid model. The five DEMs were adjusted to this geoid model to ensure statistical comparison among them.

2.3.1. Processing of the Photogrammetric DTM

The DTM was computed from aerial images using rigorous photogrammetric data reduction steps built into "Inpho DTMaster Version 7.0 software" [40]. The initial phase requires input of camera calibration parameters, flight information and aerial images. The second phase determines Exterior Orientation (EO) parameters from the onboard GPS-based camera position coordinates; Inertial Measurement Unit (IMU) derived from camera attitude (yaw, pitch, roll) and GCPs. The final phase employs a rigorous least-squares adjustment technique to compute EO parameters. Later, a regular grid of DEM was synthesized from a 3D point cloud data obtained from least-squares adjusted data. Furthermore, a DTM was generated at a spatial resolution of 10 m by removing natural and artificial features from the DEM. In this case, we edited and corrected height errors of the digging points (underestimated heights), floating points (overestimated heights), misrepresentation of terrain features such as gorges and rivers due to shadow on aerial photos, and height data of primary surfaces such as building and vegetation. This makes our photogrammetric DTM unique compared to the global DEMs that contain height errors corresponding to the primary surfaces such as built-up and vegetated areas.

2.3.2. Datum Transformation and Adjustment

Using a more accurate vertical datum is a prime importance to maintain the original vertical accuracy of the elevation models. In our case study, all the DEMs are defined with respect to the WGS84 horizontal datum. In doing so, the photogrammetric DTM was transformed from the Clarke1880 ellipsoid (Adindan Datum) to WGS84 using the following translational equation:

$$\mathrm{Dx} = -162\ \mathrm{m}, \mathrm{Dy} = -12\ \mathrm{m}, \mathrm{Dz} = 206\ \mathrm{m} \qquad \text{(Eq. 1)}$$

With regard to vertical datum adjustment, all the elevation models are redefined with a tie to the EGM2008 geoid model. This involves the task of reducing SRTM and ASTER elevation datasets from the EGM1996 geoid to the EGM2008 geoid as well as reduction of TDX ellipsoidal heights from WGS84 to the EGM2008 geoid. In practice, the reduction of SRTM and ASTER to the EGM2008 geoid will eliminate inherent errors in the EGM1996 geoid heights that reach from 0.5 to 1.0 m globally [41]. The EGM2008 geoid heights recover features from 40,000 km down to 18 km wavelengths, corresponding to a spatial resolution of 9 km and an accuracy of 15 cm globally [42]. In the territory of Ethiopia, the EGM2008 geoid model incorporates a detailed local airborne gravity data and it has better accuracy (~3.9 cm) compared to its global error budget [10]. In practice, it is highly recommended to reduce the DEMs to a more accurate vertical datum like the EGM2008 geoid in order to ensure effective utilization of the datasets for various applications.

The reduction of SRTM and ASTER to the EGM2008 geoid model involves a two-stage computation. The first phase synthesizes geoid heights from the spherical harmonic coefficients of the 1996 Earth Gravity Model (EGM1996). EGM1996 geoid heights representing features with a spatial resolution of 55 km [43] are then added to SRTM and ASTER orthometric heights to give SRTM and ASTER-based ellipsoidal heights above WGS1984 (Equation 2).

$$\mathrm{h}_{\mathrm{WGS84}} = \mathrm{H}_{\mathrm{egm96}} + \mathrm{N}_{\mathrm{egm96}} \qquad \text{(Eq. 2)}$$

Preprints (www.preprints.org) | NOT PEER-REVIEWED | Posted: 2 September 2020 doi:10.20944/preprints202009.0034.v1

Equation 3 gives the fundamental formula for computing the geoid using spherical harmonic synthesis. Various theories of geoid computation can be obtained from many literature sources [10, 44, 45].

$$N(\vartheta,\lambda) = \frac{GM}{a\gamma}\sum_{n=0}^{N}\left(\frac{a}{R(\vartheta)}\right)^{n+1}\sum_{m=0}^{n}(c_n^m cosm\lambda + s_n^m sinm\lambda)P_n^m(cos\vartheta) \qquad \text{(Eq. 3)}$$

Where, G is Newton's Universal Gravitation constant; M is mass of the Earth; a is semi-major axis of the reference ellipsoid; ϑ is the geocentric colatitude; R is mean earth radius as a function of geocentric co-latitude; n is degree of spherical harmonics; m is order of spherical harmonics; λ is longitude; R is geocentric distance; $P_n^m(\cos\theta)$ is Associated Legendre function, γ is a mean normal gravity on the reference ellipsoid.

The second phase subtracts EGM2008 geoid heights from ellipsoidal heights as computed in equation 3 to give SRTM or ASTER derived orthometric heights that are defined with reference to the EGM2008 geoid model. Similarly, TDX was also reduced to EGM2008 geoid using Equation 4.

$$\mathrm{H_{egm2008}} = \mathrm{h_{WGS84}} - \mathrm{N_{egm2008}} \qquad \text{(Eq. 4)}$$

On the other hand, the photogrammetric DTM was originally defined with respect to leveled height that was in turn defined with a tie to a historical tide gauge station located at the Port of Alexandria; via the Blue Nile first order geodetic leveling project. The second order geodetic control point derived from the Blue Nile first order geodetic leveling network was used as a vertical reference height for defining orthometric heights of the photogrammetric DTM in the study area via static DGNSS ellipsoidal heights of the Ground Control Points. This approach assumes constant vertical distance offset between WGS84 and the AMSL leveling datum-it ignores noticeable vertical separation between the geoid and the AMSL. In order to properly redefine the photogrammetric DTM rigorously from the AMSL to the EGM2008 geoid we first computed the difference between the ellipsoidal height of the second order geodetic control point (latitude 13.523958^0 N, longitude 39.553053^0 E, ellipsoidal height 2348.088 m, the AMSL height 2348.572 m) and the leveled height. This gives a vertical distance separation of -0.484 m between the AMSL datum at the Port of Alexander as computed from the second order geodetic control point and the WGS84 reference ellipsoid. The negative sign indicates that the AMSL is below the reference ellipsoid as well as it is above the EGM2008 geoid by 0.323 m.

Adding the vertical distance separation between the WGS84 and the AMSL (-0.484 m) to the leveled heights of the photogrammetric DTM that was initially determined with a tie to the AMSL reduces the DTM to the WGS84. In this stage, the photogrammetric DTM is defined in terms of ellipsoidal heights. The last stage, re-defined the ellipsoidal heights of the photogrammetric DTM to the EGM2008 geoid model by subtracting the geoid heights from it. This rigorous adjustment applied to the photogrammetric DTM allowed us to recover vertical distance separation of 0.323 m between the EGM2008 geoid and the AMSL as well as recovered unmodeled geoid undulations that were initially ignored in the computed DTM defined with reference to the AMSL. The modeled local variation of the EGM2008 geoid heights across the study area varies from -1.162 to -0.618 m with a mean and standard deviation of -0.944 m and 0.122 m, respectively. After the photogrammetric DTM data is adjusted to the EGM2008 geoid, EGM2008 geoid heights were subtracted from RTK-GNSS based ellipsoidal heights to give consistent orthometric heights that serve as ground truth data for evaluating the accuracies of the elevation models.

2.3.3. Vertical Accuracy Assessment

Although different interpolation techniques and algorithms are available, the DEM products were compared with one another using bicubic interpolation technique [46]. This is because as argued by Ghandehari et al. [47], bi-cubic interpolation technique is much suitable in recovering the sub-pixel variations of elevation of a reference in-situ random points that will be located at an off-centroid of pixels specifically in rugged terrain. First, the five DEMs (the Photogrammetric DTM, SRTM1, SRTM3, ASTER and TDX) were compared against RTK-GNSS based ground truth data. Comparison was made along six height profiles representing the different land use and land cover types and the complex topographic nature of the area (Tables 5 and 6). Secondly, a pixel-by-pixel based statistical comparison was made between the SRTM1, SRTM3, ASTER and TDX DEMs products against the high-resolution photogrammetric DTM data. More specifically, a vertical accuracy assessment was made in terms of statistical minimum, maximum, mean difference (bias), standard deviation, RMSE and Linear Error at 95% confidence interval (Equations 5-9). Finally, accuracies of the elevation models were examined against the ASPRS 2013 and 2015 standards [48, 49] and the Ethiopian standards and directives.

$$\mathrm{bias} = \frac{\sum_1^n \left(H_i^{GPS} - H_i^{DEM}\right)}{n} \quad (5)$$

$$\sigma = \sqrt{\frac{1}{n-1}\sum_{i=1}^{n}(H_i - H)^2} \quad (6)$$

$$\mathrm{RMSE} = \sqrt{\frac{n-1}{n}\sigma^2 + \mathrm{bias}^2} \quad (7)$$

$$\mathrm{LE}\ 90\% = 1.6449 \times \mathrm{RMSE} \quad (8)$$

$$\mathrm{LE}\ 95\% = 1.96 \times \mathrm{RMSE} \quad (9)$$

Where bias is mean difference, σ is standard deviation, RMSE is root mean square error, LE 90% is Linear Error (LE) at 90% two-sided confidence level and LE 95% is Linear Error at 95% two-sided confidence level.

3. Results

3.1. Vertical Accuracy of Photogrammetric Measurements

The qualities of the photogrammetric DTM as well as the performance of the other four global DEMs (two SRTMs, ASTER and TDX) against GPS derived orthometric height are analyzed and presented. The output of the processed aerial photographs showed that the geometric accuracy of aerial photos is improved by reducing uncertainty in exterior orientation parameters through utilizing accurate Ground Control Points (GCPs) and attitude of aircraft in a block adjustment computation of aerial triangulation. The results of the block adjustment corrections from the GCPs were 0.021 m, 0.006 m and 0.008 m, respectively, in the north, east and up-coordinates in terms of root mean square error (RMSE). The final photogrammetric datasets subjected to correction from the GCPs were accurate to decimeter level (as evaluated at 5 check points). The computed RMSE values are 0.537 m, 0.394 m and 0.227 m, respectively, in the north, east and up-coordinates.

3.2. Point-based *Validation of DEMs*

In this section, we presented the output of point-based accuracy of a photogrammetrically derived DTM, 1arc second and 3 arc seconds SRTM, ASTER and TDX DEM products against in-situ orthometric heights computed from EGM2008 geoid model and GNSS based ellipsoidal heights. Orthometric height is estimated from the five elevation models at the GNSS measurement points, and Table 3 presents the vertical accuracies of the five DEMs against orthometric heights derived from in-situ RTK GNSS tracked datasets and EGM2008 geoid model. The residuals between the orthometric heights (collected along six

GNSS height profiles) and five elevation models showed the relative accuracies of the models. Generally, the photogrammetric DTM agrees well with the ground truth reference datasets compared to ASTER, SRTM1, SRTM3 and TDX. The computed value of the photogrammetric DTM confirmed that it has the lowest RMSE (0.85 m); overestimating the ground truth heights with a bias of 0.69 m.

Table 3. Orthometric height difference between GNSS (H)-based orthometric height and five elevation models including A, S1, S3, P and TDX with reference to the 2008 geoid model (using 2130 point values, unit: m).

DEMs	Statistics				
	Mean	Stdev	RMSE	Min	Max
H	2213.32	137.36		1969.24	2409.57
A	2211.41	132.54		1957.35	2405.92
S3	2218.18	136.28		1969.51	2411.23
P	2214.01	137.45		1969.4	2410.62
S1	2214.62	135.95		1968.17	2410.40
TDX	2213.59	135.39		1969.57	2408.90
A – H	-1.91	14.65	14.77	-48.23	64.52
S3 – H	4.85	5.38	7.24	-25.97	33.37
S1 – H	3.45	3.16	4.68	-9.13	21.91
P – H	0.69	0.51	0.85	-2.24	5.28
TDX – H	1.30	6.12	6.26	-23.91	43.51

Legend: H = GNSS height values; A = ASTER DEM; P = Photogrammetric DTM; S3 = SRTM3 arc seconds; S1 = SRTM1 arc seconds; and TDX=TanDEM-X.

Similarly, the SRTM3 DEM agrees with the ground truth reference data compared to ASTER DEM (RMSE 14.77 m). The SRTM3 DEM has a RMSE of 7.24 m, while the vertical accuracy of the SRTM1 DEM (RMSE of 4.68 m) exceeds that of ASTER (14.77m), SRTM3 (7.24 m) and TDX (6.26 m). In the study area, TDX is the second most accurate global DEMs next to SRTM1. It has better vertical accuracy than ASTER and SRTM3. The TDX DEM has a RMSE of 6.26 m when compared to the in-situ orthometric height computed from GNSS ellipsoidal height and EGM2008 geoid height. In general, SRTM1, SRTM3, ASTER DEM, TDX and the photogrammetric DTM statistically and systematically deviate from ground truth GNSS-based tracked points by 3.45 m, 4.85 m and -1.91 m, 1.30 m, and 0.69 m, in the same order. The statistical analysis in reference to *in-situ* data indicates highest performance of the photogrammetric DTM compared to SRTM1 and SRTM3, ASTER and TDX. In this regard, however, the photogrammetric DTM, the two SRTM models, and TDX overestimate the heights, while the ASTER DEM underestimates the elevation values (Table 3). In addition, in more practical terms, Table 4 shows the absolute vertical accuracy of the photogrammetric DTM and the four digital elevation models used in this study. In reference to in-situ orthometric heights, the absolute vertical accuracy of the photogrammetric DTM (1.67 m at LE 95%) is almost an order of magnitude better than that of TDX, SRTM3 and ASTER DEMs. With a better statistical rigorous and geographic completeness, the absolute vertical accuracies of the TDX, SRTM1 and SRTM3 in relation to the photogrammetric DTM perform better than their respective product specification accuracies. In contrast, the absolute vertical accuracy of the ASTER DEM does not meet its product specification accuracy in the study area.

Table 4. A) Linear error of the elevation models in reference to orthometric height derived from RTK GNSS ellipsoidal heights and EGM2008 geoid and **B)** Linear error of the global elevation models in reference to photogrammetric DTM at 95% and 90% confidence level (LE 95%=1.96x RMSEz, LE 90%=1.6449x RMSEz). LE are estimated according to the NSSDA and NMAS standards.

	A) linear error of the elevation models in reference to RTK GNSS ellipsoidal heights		B) Linear error of the elevation models in reference to photogrammetric DTM	
Elevation data	NSSDA (95%)	NAMS (90%)	NSSDA (95%)	NAMS (90%)
P	1.67	1.40	-	-
A	28.95	24.30	24.11	20.23
S1	9.17	7.70	5.86	4.92
S3	14.19	11.91	9.13	7.67
TDX	12.26	10.29	4.46	3.74

NB: Refer to the abbreviations in Tables 3.

3.3. Grid-based Comparison of the Global Elevation Models against Photogrammetric DTM

Vertical accuracies of the four global elevation models were presented in relation to that of the local photogrammetric DTM. Height differences between the elevation models were statistically analyzed on a pixel-by-pixel basis. Prior to grid based accuracy evaluation, SRTM1, ASTER and photogrammetric DTM were re-sampled to 90 m resolution (cell size) using bicubic interpolation techniques to make them consistent with the 90 m spatial resolution of SRTM3 and TDX [50]. In connection to this, the residual orthometric heights between the reference elevations model (derived from ultra-high resolution of re-sampled photogrammetric DTM) and re-sampled SRTM1 and ASTER, as well as the SRTM3 and TanDEN-X 90m are presented in Table 5.

Table 5. Orthometric height differences between photogrammetric DTM and the four global elevation models with reference to the 2008 geoid model (using 36,000 point values), unit: m.

DEMs	Statistics				
	Mean	Stdev	RMSE	Min	Max
P	2179.16	135.22	-	1905.23	2516.33
A	2176.03	132.98	-	1890.27	2530.64
S3	2180.91	135.24	-	1907.38	2515.71
S1	2180.65	135.14	-	1905.53	2516.69
TDX	2178.27	134.88	-	1906.13	2513.62
A – P	-3.13	11.90	12.30	-149.35	110.65
S3 – P	1.75	4.32	4.66	-48.78	55.06
S1 – P	1.49	2.59	2.99	-34.69	46.5
TDX – P	-0.89	2.09	2.28	-34.20	34.95

NB: Refer to the abbreviations in Table 3.

The statistics in Table 5 are showing the difference among the four elevation models against the photogrammetric derived DTM. Our results indicated that a very good agreement is observed between photogrammetric DTM and TDX; and their difference has a RMSE of 2.28 m and bias of -0.89 m. In addition, the two SRTM elevation models have good agreement with the photogrammetric DTM. The

Preprints (www.preprints.org) | NOT PEER-REVIEWED | Posted: 2 September 2020 doi:10.20944/preprints202009.0034.v1

SRTM1 has a RMSE of 2.99 m and bias of 1.49 m, while the SRTM3 has a RMSE of 4.66 m and bias of 1.75 m. On the other hand, the residuals between photogrammetric DTM and ASTER are significant across the whole study area (Figure 2). As clearly presented in Table 5, the residuals between the photogrammetric DTM and ASTER DEM have a RMSE of 12.30 m and the maximum value reaches up to -149.35 m. The residuals between the two models have a bias of -3.13 m, meaning ASTER underestimates heights compared to the photogrammetric DTM. In general, from the four global digital elevation models TDX has a very good agreement with photogrammetric DTM than other elevation models (Table 5).

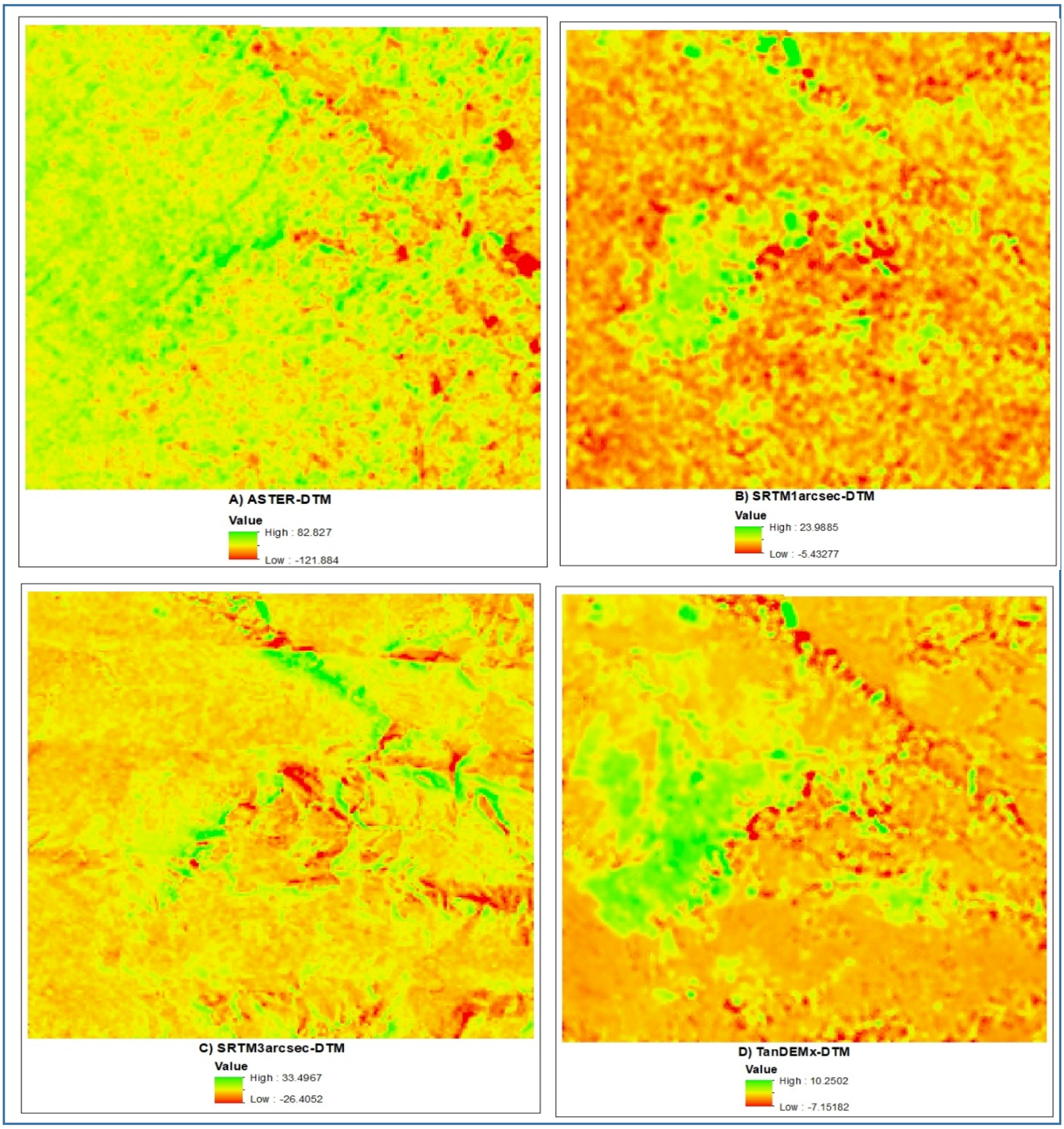

Figure 2. (A) Presents pixel based deviation map of ASTER DEM from photogrammetric DTM (**A** − **P**); (B) presents pixel based deviation map of SRTM1 from photogrammetric DTM (**S1** − **P**); (C) presents pixel based deviation map of SRTM3 from photogrammetric DTM (**S3** − **P**) and (D) presents pixel based deviation map of TanDEM-X from photogrammetric DTM (TDX − **P**), Map (unit: m).

Moreover, the computed results of SRTM elevation models and TDX mimic to the photogrammetric DTM almost across highlands and low lands, situated in the central depression, northern and southern plateaus of the study site. It is also observed that the vertical accuracy of the three elevation models (SRTM1, SRTM3 and TDX) models agreed well with photogrammetric DTM across the central and northeastern parts of the study area (Figure 2), which is being characterized by extremely rugged terrain. However, this study showed significant deviation of each of the four elevation models from the photogrammetric DTM, specifically in areas that are characterized by high slopes and extremely undulating terrain (Figure 3). The differences are strongly correlated with escarpments, tributaries, dissected topography and gullies. Particularly, the differences are noticeable in north eastern, central and eastern, and southern parts of the study area (Figure 2). In these areas, the difference between the SRTM elevation models (SRTM1 and SRTM3) and photogrammetric DTM are significant, and the orthometric height values of SRTM elevation models are greater than those of photogrammetric DTM mainly along the escarpment. The reverse is true in areas that are characterized by river or drainage systems and dissected topography. This may be related to limitations of the interferometric technique to acquire accurate data over extremely rugged topography that is characterized by high slopes, and height variations.

3.4. Vertical Accuracy across Different Land Use and Land Cover Types

In theory, the accuracy of the elevation models are also sensitive to the characteristics of ground targets or land use/land cover types. In this regard, comparison was made using GNSS survey profiles (Figure3 1 and 3) to observe how the accuracies the different digital elevation models' are sensitive to the different land use land cover types.

Table 6. The minimum and maximum values of the five DEMs against GNSS derived orthometric height profiles surveyed across different land use land cover types (vertical datum is geoid2008 and unit: m).

	P	A	S3	S1	Tx	P	A	S3	S1	Tx
Land use Types	Min	Min	Min	Min	Min	Max	Max	Max	Max	Max
Sparse trees	-5.28	-36.17	-29.66	-16.74	-19.85	1.72	38.56	25.97	9.06	20.03
Road alignment	-2. 42	-37.36	-19.87	-17.00	-11.21	1.06	24.24	2.74	2.29	5.96
Drainage pattern	-2.8	-64.52	-33.37	-21.91	-33.13	2.24	43.04	7.26	9.23	3.13
Farm land	-2.75	-14.73	-26.19	-13.01	-12.19	1.65	48.23	20.27	5.43	16.27
Built-up areas	-1. 42	-30.96	-10.81	-6.99	-3.86	0.18	16.92	8.67	2.08	5.74
Bare lands	-1.6	-16.02	-7. 48	-6.64	-2.82	-0.07	33. 47	1.38	1.74	1.96

NB: Refer to the abbreviations in Table 3 and Figure 1.

Accordingly, we found that the agreement between elevation models and ground truth reference datasets vary from profile to profile depending on variation in land use/land cover types. Tables 6 and 7 show the quantitative comparison of the five elevation models against orthometric heights acquired along six GNSS survey profiles representing different land use and land cover types. The statistical analysis in reference to GNSS tracked dataset indicates highest performance of the photogrammetric DTM compared to SRTM1, SRTM3, ASTER and TDX. The RMSE of the SRTM1 and SRTM3, ASTER and TDX also showed noticeable variation across the six elevation profiles. The mismatch between photogrammetric and GNSS tracked dataset varies from 0.49 m (in farmlands) to 0.89 m (in sparse tree areas) in terms of RMSE. Moreover, as clearly indicated in Table 7, the RMSE of SRTM1 and SRTM3, ASTER and TDX, ranges from 2.65 (in bare lands) to 6 m (along drainage patterns), 1.76 m (in farm lands) to 2.93 m (sparse tree areas), 2.81m (in farm lands) to 15.6m (in bare lands) and 0.91 m (in bare

Preprints (www.preprints.org) | NOT PEER-REVIEWED | Posted: 2 September 2020 doi:10.20944/preprints202009.0034.v1

lands) to 6.19 m (in drainage pattern areas), respectively. In general, along every GNSS survey profile, photogrammetric DTM showed strong correlation with the ground-truth data as compared to SRTM1and SRTM3, ASTER and TDX.

Table 7. Descriptive Statistics for vertical error for the five DEMs by land cover (vertical datum is geoid2008 and unit: m).

Land use Types	P	A	S3	S1	TX	P	A	S3	S1	Tx
	Mean					RMSE				
Sparse Trees	-0.63	-10.00	-9.65	-4.15	0.04	0.89	3.67	2.93	5.73	5.46
Road alignment	-0.56	-4.75	-4.53	-3.45	-1.27	0.59	3.87	2.10	4.70	3.18
Drainage Pattern	-0.60	-3.36	-6.51	-4.66	-3.76	0.81	5.54	2.35	6.00	6.19
Farm land	-0.79	10.19	-2.83	-2.50	0.68	0.49	2.81	1.76	3.14	1.97
Built Up Areas	-0.59	2.54	-3.08	-3.00	-0.08	0.54	3.10	1.91	3.63	1.86
Bare Lands	-0.86	13.16	-2.15	-2.04	0.41	0.88	15.60	2.65	2.65	0.91

NB: Refer to the abbreviations in Table 3.

3.5. Vertical Accuracy across Different Slope Classes

The vertical accuracies of the elevation models are further assessed by slope to examine the sensitivity of vertical errors across to different terrain (slope) characteristics across the study area. The slope is derived from the re-sampled photogrammetric DTM at 90 m spatial resolution, and classified into 7 slope categories and Hawker et al. [25] proposed slope classification scheme was adopted (Figure 3).

Table 8. Vertical error in RMSE of the DEMs in reference to in-situ-based measured orthometric heights against by different slope classes (Unit: m).

Slope (°)	0-0.5	0.5-1	1-3	3-6	6-10	10-15	15+
Description	**Flat**	**Nearly flat**	**Very gentle slope**	**Gentle slope**	**Moderate slope**	**Steep slope**	**Very steep slope**
ASTER	12.83	9.89	12.60	15.17	13.91	20.34	19.62
SRTM3	6.03	4.32	4.39	5.35	7.44	10.42	15.50
SRTM1	4.05	3.75	3.69	4.00	4.99	6.60	7.65
TDX	4.35	2.39	2.33	3.06	4.46	7.03	8.58
Photogrammetric DTM	0.80	0.78	0.82	0.85	0.81	0.86	1.09
No. of GNSS tracked points	49	89	887	531	224	166	190

Table 8 presents the distribution of vertical errors of the elevation models as compared to in-situ orthometric heights. Overall, in reference to the orthometric heights, the photogrammetric DTM has a better vertical accuracy for all slope categories as compared to ASTER, SRTM3, SRTM1 and TDX DEMs. In connection to this, the vertical errors of all DEMs computed in relation to the orthometric heights increase linearly as a function of slope. Some of DEMs have lower RMSE for flat to gentle slopes and largest values for the steepest slopes. In particular, the RMSE values of ASTER and SRTM3 DEMs increase considerably for ‘moderate slopes’, ‘steep slopes’ and ‘very steep slopes’.

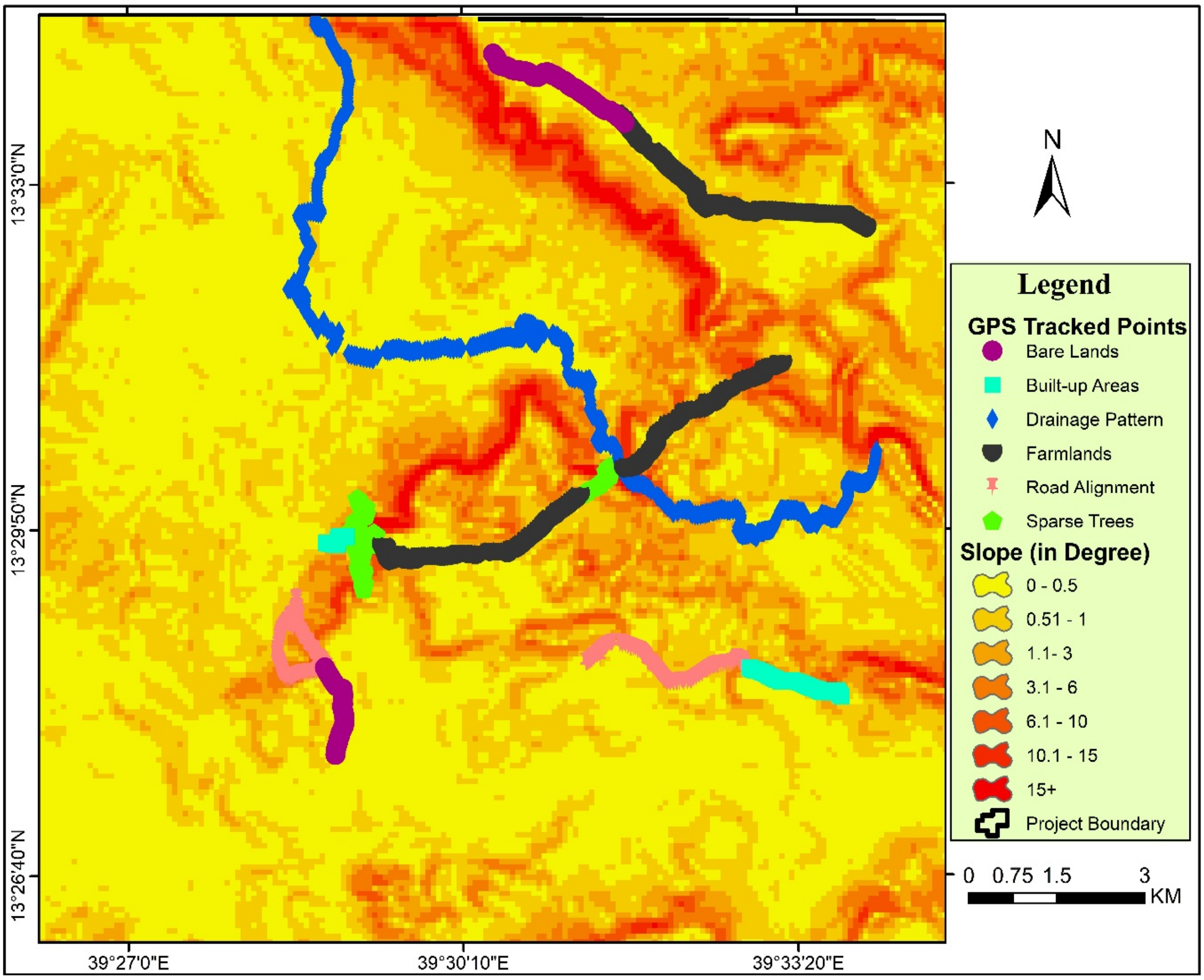

Figure 3. Routes and profiles of the surveyed elevation data located across the study area, and detailed description of the profiles are presented in Table 2.

While the vertical error of the photogrammetric DEM is lowest (Table 8 and Figure 3) for all slope classes and this is due to the removal of natural and man-made features from the photogrammetric DEM during DTM editing process. TDX and SRTM1 have almost the same level of vertical accuracies across different slope categories. On the contrary, SRTM1 slightly performs better accuracy than TDX product in 'flat', 'steep' and very steep slopes', while TDX has the lowest RMSE for the remaining slope categories. In general, for all slope categories, both SRTM1 and TDX are more accurate than SRTM3 and ASTER DEMs The vertical errors of SRTM3 and ASTER increase considerably for slope values larger than 10°. As a whole, our results show that the vertical accuracy of the elevation models are strongly associated with terrain slope.

Similarly, the vertical accuracies of the global DEMs (i.e. SRTM1 and SRTM3, ASTER and TDX) are evaluated against photogrammetric DTM as a function of terrain slope, and accuracy assessment was made across the study area using different slope classes. Figure 4 shows the vertical errors (RMSE) distribution of the global DEMs (i.e., SRTM1, SRTM3, ASTER and TDX) by slope classes as evaluated against the photogrammetric DTM. TDX has the lowest values of RMSE than SRTM1, SRTM3 and ASTER products for all slope classes, demonstrating its superiority across the study area terrain characteristics. In this regard, Rexer and Hirt [51] also argued that also the quality of SRTM is superior to the global ASTER elevation model. Besides, the vertical accuracy of SRTM1 is almost equivalent to that of TDX DEM. In addition, SRTM3 data is slightly better than SRTM1 for 'flat', 'nearly flat' and 'very gentle' slopes, while SRTM1 surpasses SRTM3 for 'gentle', 'moderate', 'steep' and 'very steep' slopes. The vertical errors of ASTER and SRTM3 increase considerably for slope values larger than 3°. Altogether, our results show that the vertical accuracies of the elevation models are strongly associated with terrain slopes. They have linear relationships in which the vertical errors of the elevation data increase as the values of the terrain slope increase.

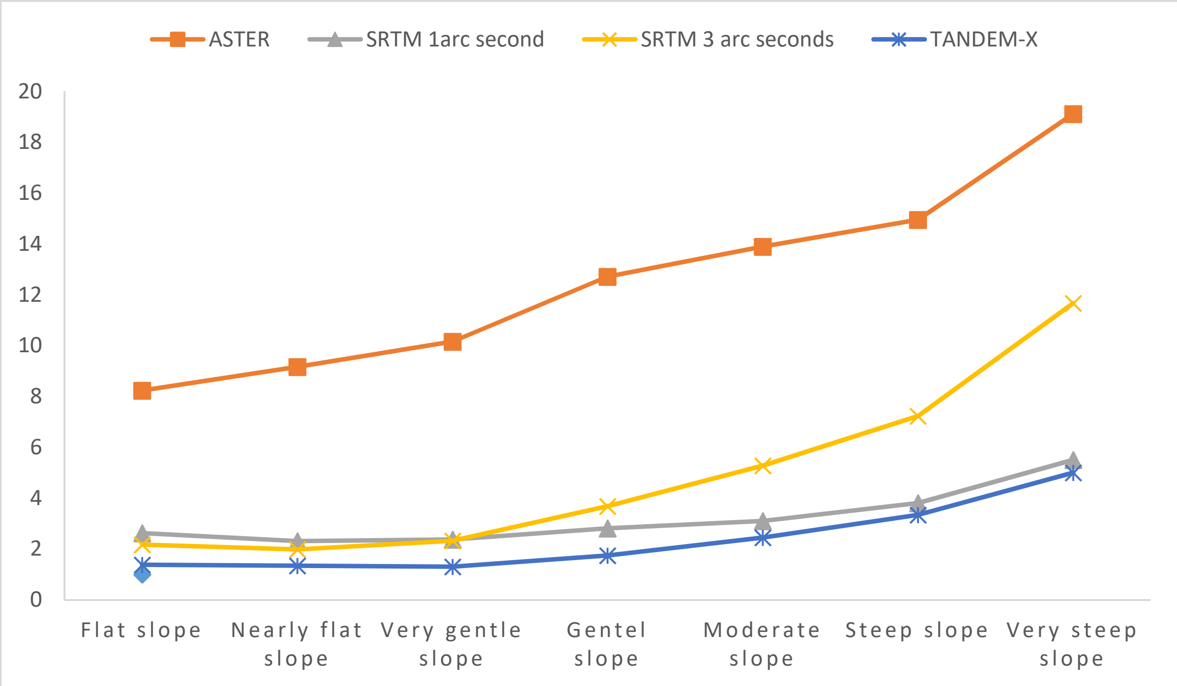

Figure 4. Density plot of RMSE of the global DEMs against the photogrammetric DTM by slope category.

4. Discussion

The accuracy of SRTM, ASTER, TDX and the photogrammetric DTM were evaluated, and the residuals between the orthometric heights and five elevation models clearly showed the relative accuracies of the models. As evidently indicated in the result section, it is understandable that the vertical accuracy of the photogrammetric data (0.23 m) meets the ASPRS standard of 49.0 cm for non-vegetated areas and 75.0 cm for vegetated areas [48, 49]. We also have evaluated the vertical accuracies of the SRTM1 and SRTM3, ASTER and TDX that shows Linear Error (LE) computed based on ASPRS standards for the five topographic models against RTK-GNSS based orthometric heights at the 90 and 95 two-sided percentiles of confidence interval (Table 4). Based on these standards, the absolute vertical accuracy of the photogrammetric DTM is 1.67 m (LE 95%). Our analysis showed that the photogrammetric DTM best qualify the ASPRS standard [48, 49], and more specifically, based on LE 95%, the photogrammetric DTM is conformal to a 100 cm vertical accuracy class. In relation to the ground truth, the accuracy of the photogrammetric DTM (an absolute error of 1.67 m or 1 m vertical accuracy class) is lower than the quality of original data (RMSE of 0.227 m or 0.2 m vertical accuracy class) as estimated by five checkpoints and four GCPs. The increase in the absolute error comes from both photogrammetric data and ground truth data as well as limitations related to statistical rigorousness of adjustment analysis derived from few checkpoints and GCPs.

The photogrammetric products also qualify for the ASPRS [49, 52] vertical accuracy assessment standards of: i) a 33.3 cm vertical accuracy class, ii) a 65.3 cm Non-vegetated Vertical Accuracy (NAV),

iii) a 99.9 cm Vegetated Vertical Accuracy (VVA), and iv) equivalent class 1 (99.9cm) and class 2 (50 cm) contour interval (Appendix I). Although our results well substantiated the accuracy of airborne-based photogrammetric DTM and meets the well-known standards, the vertical accuracy (RMSEz = 0.85 m) of the photogrammetric DTM is slightly poorer than the expected vertical accuracy corresponding to three pixels (±0.75 m) as per the ASPRS standard [48]. This level of DEM vertical accuracy is good enough for photogrammetric data to meet many applications like rural cadaster, natural resource management, digital soil mapping, watershed management, floodplain mapping, natural disaster and risk management, infrastructure management, aviation safety, etc. However, the photogrammetric DTM produced at a spatial resolution of 10 m does not qualify for urban cadaster application that requires vertical accuracy in the order of ±0.45 m, as per the Ethiopian standard [53].

At large, the accuracy of the photogrammetric DTM best complies with in-situ-based Real-Time Kinematic GNSS tracked points compared to the other global ASTER, SRTM1, SRTM3 and TDX elevation models. In the study area, the vertical accuracy of the two SRTM elevation models surpass that of ASTER DEM. In this regard, the findings of this study coincide with previous studies that correspondingly reported the superiority of SRTM (30 m and 90 m resolution) over ASTER global elevation model [54].

In reference to in-situ orthometric heights, the SRTM product showed a better performance in our study area compared to its product specification. SRTM3 has an absolute vertical accuracy of 11.91 m (LE at 90% confidence level) that is much better than its product specification, RMSE of 9.73m (16 m absolute accuracy at 90% confidence level) [4]. This indicates that 92.02% of the SRTM3 data has an absolute error in height information smaller than 16m. This observed vertical accuracy of the SRTM in Ethiopia is better as compared to its performance reported in Polish Tatra Mountains. In Poland, SRTM3 showed conformity to its product specification accuracy of 16 m with 82% [55]. Besides, the absolute vertical accuracy of SRTM3 has significantly improved when it is compared to a regular grid of photogrammetric DTM, 7.67 m at LE 90% and 9.13 m at LE 95% (Table 4). The absolute vertical accuracy of SRTM1 (7.70 m and 9.17 m, respectively at LE 90% and LE 95%) in reference to in-situ orthometric heights is remarkably better than that of the SRTM3 data.

The SRTM1 product showed noticeable improvement when compared to the accuracy of the SRTM3 product specification. Most of the errors (96.2%) in the height values of the SRTM1 DEM are smaller than RMSE of 9.73 m (SRTM product specification absolute vertical accuracy of 16 m) as compared to 92.02% of the SRTM3. In contrast to SRTM, the absolute accuracy of ASTER is lower than the accuracy reported in its product specification. The absolute accuracy of ASTER-GDEM version 2 in reference to *in-situ* orthometric heights (28.95 m at LE 95% confidence level) is low compared to its design goal of 17 m absolute accuracy at LE 95%, which is equivalent to RMSE of 8.67 m [54]. This corresponds to larger error budget in the ASTER elevation model. In the study area, only 48.5% of the elevation values of the ASTER DEM has smaller error budget than the SRTM3 product specification vertical accuracy, demonstrating its low performance. The observed accuracies of SRTM3 and ASTER DEMs in our study area have showed slightly better accuracies (SRTM 13.73 m, ASTER 20.07m at LE 95%, Table 4) than the findings of the study conducted in Tokyo [28]. The difference may be caused by variation in topography.

On the other hand, the vertical accuracy of the TDX DEM is comparable to that of SRTM1 when compared in reference to in-situ orthometric heights. In this comparison, the absolute vertical accuracy of the TDX at LE 90% (10.29 m) is almost equivalent to its product specification of 10 m. As clearly indicated in the results section, it has also even better absolute vertical accuracy of 3.74m at LE 90% when compared to the photogrammetric DTM (Table 4B). Overall, in reference to the photogrammetric DTM (Table 4B), the quality of TDX data is slightly better than SRTM1 and remarkably better than SRTM3 [28, 49]. Moreover, the accuracy of ASTER with respect to photogrammetric data covering in the study area is also relatively lower (24.11 m at LE 95%) than its product specification (i.e., an absolute vertical accuracy of 17 m) [30, 31]. Largely, our findings confirmed a better performance of TDX, SRTM1 and SRTM3 than ASTER. While other previous studies asserted that, the photogrammetric DTM has shown an extraordinary accuracy (1.67 m at LE 95% and 1.40 m at LE 90%) compared to the findings of other global digital elevation models [45]. In addition to vertical accuracy, the photogrammetric data also agree with the ASPRS's horizontal accuracy requirements and it has a horizontal accuracy of 0.54 m and 0.39 m in the northing and easting, respectively, in terms of RMSE compared to the ASPRS desired accuracy of 0.613 m (2.45xGSD at 95% confidence level, with the photogrammetric data has a ground sampling distance of 25 cm) [48, 49].

The quality of digital elevation models also varies across the different land use/land cover types and terrain characteristics. These findings also supported by Gdulová et al. [56] conclusive argument. The RMSE of the SRTM1 and SRTM3, ASTER and TDX showed noticeable variation across the six land use land cover types. Our results showed higher errors in areas that are characterized by a drainage pattern land cover (Profile-3), sparse tree areas (Profile-1) and in bare land topography (Profile-6). The accuracy of ASTER is lower in the drainage patterns and bare lands, while that of SRTM is low in sparse tree areas and along bare lands. This is probably because the C-band radar used by the SRTM is not fully capable to penetrate through vegetation canopy. In this regard, studies like Tachikawa et al. [54] showed the low accuracy of satellite stereoscopic observation in areas where covered with thick vegetation canopy. Wessel et al. [39] also indicated low accuracy of TDX across vegetated areas, which is in agreement with our results. Besides, in line with the digital elevation model vertical accuracy assessment in vegetation areas, our finding is complemented with the findings of Hawker et al.[25], and they argued that TDX is the most accurate global DEM in all land cover types tested except short vegetation and tree-covered areas.

With regard to validation analysis of the different DEMs across topographic (slope) characteristics, the two elevation models (SRTM1 and TDX) agreed well with photogrammetric DTM for all slope classes. The error of TDX is marginally lower than SRTM 1arcsecond for all slope categories. The SRTM3 conforms well to the photogrammetric DTM across topographic landmasses characterized by lower slope angles. In contrast to other elevation models, ASTER DEM significantly deviates from the photogrammetric DTM across almost all slope classes. For all global DEMs used in this study, the lowest RMSE values are found in gentle slope areas. For ASTER and SRTM 3 arc seconds, RMSE values increase considerably for slopes larger than 10° ('steep' and 'very steep slopes'), while this change is less for TDX and SRTM1. Wessel et al. [39,57] also found a considerable rise in RMSE values above slopes of 10° ('steep slope'), however, our analysis differs slightly from this findings and bin all slopes below 10° into 1 category while we separate into 5 bins below 10° owing to our focus on gentle slope terrain. This may be related to limitations of the interferometric technique to acquire accurate data over extremely rugged topography that is characterized by high slopes and height variations. In such topographic, the radar beam is not able to illuminate all portions of the ground surface; radar cannot see topographic masses that are occluded from its view. The low backscattered power of radar signals from some "shadow" regions causes random error in the interferometric phase [58] and thus the resulting heights from the observed phases are affected by larger errors. Besides, due to the side-looking geometry of radar satellites, the layover effect is assumed significant in terrain areas where variation in elevation exceeds 1.8m per pixel [51]. In general, the compressed layover in the slant range geometry has a larger component in the direction of ground range and therefore introduces errors in height information.

5. Conclusions

The quality of any spatial data needs to be validated by carrying out an in-depth accuracy assessment before using the products for different applications. Thus, the objective of this study was to evaluate the vertical accuracy of aerial photogrammetric DTM and four global digital elevation models against in-situ orthometric heights derived from ellipsoidal heights and the EGM2008 geoid heights on the one hand, and assessing the quality of the four global digital elevation models against the aerial photogrammetric DTM measurements from the other. We used different sources of datasets including ASTER, SRTM3, SRTM1 and TDX DEMs as well as Kinematic GNSS tracked point datasets (2130 validation points) acquired from static Differential Global Navigation Satellite Systems (DGNSS) geodetic positioning using dual-frequency receivers. Accordingly, the accuracy of the photogrammetric DTM made available to us is convincingly in agreement with the ASPRS and Ethiopian Mapping Agency's standards. The photogrammetric DTM is also observed to be more accurate when compared to SRTM1 and SRTM3, ASTER and TDX. The DTM has an absolute vertical error of 1.67 m at LE 95% confidence level, meeting the 100 cm vertical accuracy class of the ASPRS standard.

Comparing to orthometric heights derived from RTK GNSS based ground truth ellipsoidal heights and EGM2008 geoid, the accuracy of SRTM3 is considerably better than ASTER, and its absolute elevation error is lower than the product specification of 16 m absolute accuracy at LE 90%. Besides, in reference to in-situ orthometric heights, the accuracy of SRTM1exceeds the accuracy of the other three global DEMs, i.e. ASTER, SRTM3 and TDX. Moreover, SRTM1 and SRTM3 as well as TDX showed better accuracy than ASTER when compared to the photogrammetric DTM across an area of approximately 298 km^2, based on pixel-by-pixel comparison. The SRTM elevation models (SRTM1 and SRTM3) noticeably deviate from photogrammetric DTM in areas characterized by undulating terrain. In relatively flat areas, the two elevation models are in a good agreement. Similarly, ASTER DEM considerably deviate from the photogrammetric DTM than the SRTM elevation models. The residuals between ASTER and the photogrammetric DTM have significant differences in all areas; however, the mismatch is larger in areas of steep slope. The discrepancy may be attributed to shadow and layover effects of the C-band radar signal and low resolution of satellite stereoscopic view compared to high-resolution aerial stereo images. When compared to the photogrammetric DTM, TDX has better accuracy than the SRTM elevation models and ASTER DEM.

The study also showed the importance of reducing the elevation models to a more accurate local geoid, in view of preserving the actual accuracy of the resulting DEMs or DTMs. We also found that referring to the local AMSL datum would ignore significant variation of the local geoid model. In this study, the EGM2008 geoid model differs from the AMSL datum by an amount ranging from -1.162 m to -0.618 m with a mean and standard deviation of -0.944 m and 0.122 m, respectively. Therefore, before using any application, it is highly recommended to reduce the elevation models to a very accurate local geoid model to reduce errors. Besides, further accuracy assessment studies are required to evaluate the photogrammetric DTM using integration of static GNSS and Network-Based RTK GNSS measurement. It is also important to compare the photogrammetric DTM against elevation data that can be locally computed from remotely sensed radar images or LiDAR data. Finally, the finding of the study confirmed that topographic datasets such as the photogrammetric DTM, TDX and SRTM1 digital elevation models would play a unique role for earth sciences, environmental research, urban planning, positioning and navigation services, environmental disaster monitoring and management plans, defense and security applications in a country like Ethiopia having scarce high resolution spatial datasets and very rugged topography.

Author Contributions: **T.B** and **B.G** conceived and conceptually framed the research idea initially, and wrote a first draft of the manuscript, while **H.B** involved in data collection, data processing, analyzing the data and conducting this study for the partial fulfillment of her MSc thesis research under the close supervision of **T.B** and **B.G**. Besides, **T.B, B.G**, and **M.V** reviewed and edited the manuscript exhaustively as well as commenting on the results and conclusions sections of the manuscript.

Funding: This research was funded under the Entoto Observatory and Research Center, Ethiopian Space Science and Technology Institute postgraduate research fund scheme.

Acknowledgements: The authors acknowledge the United States Geological Survey for the supply of ASTER and SRTM elevation models. The authors also gratefully acknowledge Information Network Security Agency for providing GNSS receivers and deploying technical surveyors during the fieldwork. Besides, the authors thank the measurement team members mainly Yonas Teklu, Dawit Berihe, Yared Regassa, Tofiq Ali, Mesfin Archema and Mohammednur Abdela for their important contribution during the field data collection period. Finally, the authors thank anonymous reviewers of this journal for their helpful remarks.

Conflicts of Interest: The authors declare no conflict of interest.

References

1. Hipkin, R.G. Defining the geoid by W = W0 = U0: Theory and practice of a modern height system. In: Gravity and Geoid 2002, 3rd Meeting of the International Gravity and Geoid Commission, Thessaloniki, Greece **2002,** 367-377.
2. Meyer, T.H.; Roman, D.R., Zilkoski, D.B. What does height really mean? Part IV: GPS Orthometric Heighting. Surveying and Land Information Science **2006**, 66(3), 165-183.
3. Hofmann-Wellenhof, B.; Moritz, H. Physical Geodesy, **2005,** SpringerWien, Austria, pp412.
4. Farr, T.G.; Rosen, P.A.; Caro, E.; Crippen, R., Duren, R., Hensley, S., Kobrick, M., Paller, M., Rodriguez, E., Roth, L., Seal, D., Shaffer, S., Shimada, J., Umland, J., Werner, M., Oskin, M., Burbank, D. and Alsdorf, D. The Shuttle Radar Topography Mission. Reviews in Geophysics **2007**,45, 1–33.
5. Ferretti, A.; Prati, C.; Rocca, F. 'Multibaseline InSAR DEM reconstruction: the wavelet approach' Geoscience and Remote Sensing, IEEE Transactions on Geoscience and Remote Sensing, **1999**, 37(2), 705-715.
6. Bedada, T.B. An Absolute Geopotential Height System for Ethiopia, **2010,** PhD Thesis, University of Edinburgh., Edinburgh, Scotland.
7. Hipkin, R.; Haines, K.; Beggan, C.; Bingley, R.; Hernandez, F.; Holt, J.; Baker, T. The geoid EDIN2000 and mean sea surface topography around the British Isles, Geophys.J.Int. **2004**, 157, 565–577.
8. Smith, D.A.; Holmes, S.A.; Li, X.; Guillaume, S.; Wang, Y.M.; Bürki, B.; Roman, D.R.; Damiani, T.M. Confirming regional 1 cm differential geoid accuracy from airborne gravimetry: The Geoid Slope Validation Survey of 2011. J Geod. **2013**, 87:885–907. DOI 10.1007/s00190-013-0653-0.
9. Wilson J.P. Environmental Applications of digital terrain modeling, **2018,** John Wiley & Sons, Inc., USA and John Wiley & Sons Ltd, United Kingdom, pp359.

10. Lindholm, M.S.; Heyman, J. Glacial geomorphology of the Maidika region, Tibetan Plateau, Journal of Maps **2016,** 12 (5), 797-803, DOI: 10.1080/17445647.2015.1078182.
11. Baldi, P.; Bonvalot, S.; Briole, P.; Coltelli, M.; Gwinner, K.; Marsella, M.; Puglisi, G.; Rémy, D. Validation and comparison of different techniques for the derivation of digital elevation models and volcanic monitoring (Vulcano island, Italy), International Journal of Remote Sensing **2002**, 23(22), 4783-4800.
12. Kiyoshi, H.; Nagai, M. Real-time volcano activity mapping using ground-based digital imagery, ISPRS Journal of Photogrammetry and Remote Sensing **2002**, 57 (1-2), 59-168, DOI: 10.1016/S0924-2716(02)00112-0.
13. Dhakal, A.S.; Amanda, T.; Aniya, M. Landslide hazard mapping and its evaluation using GIS: an investigation of sampling schemes for a grid-cell based quantitative method. Photogramm Eng Remote Sens **2000**, 66, 981–989.
14. Mora, P.; Baldi, P.; Casula, G.; Fabris, M.; Ghirotti, M.; Mazzini, E.; Arianna, P. Global Positioning Systems and digital photogrammetry for the monitoring of mass movements: Application to the Ca' di Malta landslide (northern Apennines, Italy), Engineering Geology **2003**, 68 (1-2), 03-121, DOI: 10.1016/S0013-7952(02)00200-4.
15. Westen, V.; Getahun, L. Analyzing the evolution +of the Tessina landslide using aerial photographs and digital elevation models, Geomorphology **2003,** 54 (1-2), 77-89, DOI: 10.1016/S0169-555X(03)00057-6.
16. Arianna, P.; Baldi, P.; Bedin, A.; Casula, G.; Cenni, N.; Fabris, M.; Loddo, F.; Mora, P.; Bacchetti, M. Digital Elevation Models for landslide evolution monitoring: application on two areas located in the Reno River Valley (Italy), Annals of geophysics **2004**, 47 (4), 1339-1354, DOI: 10.4401/ag-3348.
17. Lee, S.J.; Komatitsch, D.; Huang, B.; Tromp, J. Effect of topography on seismic-wave propagation: an example from north Taiwan. Bull Seismol Soc Am. **2009**, 99, 314–325.
18. Wieczorek M.A. Gravity and topography of the terrestrial planets. Treatise on Geophysics **2007**,10, 165-205.
19. Kirby, J.; Featherstone, W. High-resolution grids of gravimetric terrain correction and complete Bouguer corrections over Australia. Exploration Geophysics **2002**, 33, 161-165.
20. Tsoulis D. Terrain correction computations for a densely sampled DTM in the Bavarian Alps. J Geod .**2001**, 75, 291-307.
21. Forsberg, R. Gravity field terrain effect computations by FFT. Bull Géod. **1985,** 59, 342-360.
22. Moudrý, V., Lecours, V., Gdulová, K., Gábor, L., Moudrá, L., Kropáček, J., & Wild, J. On the use of global DEMs in ecological modelling and the accuracy of new bare-earth DEMs. Ecological Modelling, **2018,** 383, 3-9.
23. Wang, W.; Yang, X.; and Yao, T. Evaluation of ASTER GDEM and SRTM and their suitability in hydraulic modelling of a glacial lake outburst flood in southeast Tibet. Hydrological Processes **2012**, 26(2), 213-225.
24. Taufik, M.; Putra, Y.S.; Hayati, N. The utilization of global digital elevation model for watershed management a case study: Bungbuntu Sub Watershed, Pamekasan, Procedia Environmental Sciences **2015**, 24, 297–302.
25.Hawker, L.; Neal, J.; Bates, P. Accuracy assessment of the TanDEM-X 90 Digital Elevation Model for selected floodplain sites. Remote Sensing of Environment **2019,** 232 (111319),1-15.
26. Sanecki, J.; Klewski, A.; Beczkowski, K.; Pokonieczny, K.; Stępień, G. The usage of DEM to create the 3D cadastre. Scientific Journals, **2013.** 33 (105), 86–90.
27. Pramanik, M.K. Site suitability analysis for agricultural land use of Darjeeling district using AHP and GIS techniques. Modeling Earth Systems and Environment **2016,** 2(56).1-22.
28. Avtar R.; Yunus A.P.; Kraines S.; Yamamuro M., Evaluation of DEM generation based on Interferometric SAR using TanDEM-X data in Tokyo, Physics and Chemistry of the Earth, Parts A/B/C **2015**, 83–84,166-177
29. Lee, I.; Chang, H.C.; Ge, L. GPS Campaigns for Validation of InSAR Derived DEMs. Journal of Global Positioning Systems **2005**, 4 (1-2), 82-87.
30.ASTER GDEM Validation Team. ASTER Global DEM Validation Summary Report **2009** p.http://www.ersdac.or.jp/GDEM/E/image/ASTERGDEM_Validation"http://www.ersdac.or.jp/GDEM/E/image /ASTERGDEM_ValidationSummaryReport_Ver1.pdf, 2009. (Retrieved on 5 June 2018).
31. ASTER GDEM Validation Team, ASTER Global Digital Elevation Model Version 2 Summary of Validation Results. 2011. HYPERLINK "https:// igskmncnwb 001. cr.usgs.gov/aster /GDEM/ Summaryhttps:// igskmncnwb 001. cr.usgs.gov/aster/GDEM/SummaryGDEM2_validation_report_final.pdf(Retrieved on 5 June 2018).
32. Berry, P.A.M.; Garlick, J.D.; Smith, R.G. Near-global validation of the SRTM DEM using satellite radar altimetry. Remote Sensing of Environment **2007,** 106(1), 17-27.
33. Hirt, C., Filmer, M.S, Featherstone, W.E. Comparison and validation of the recent freely available ASTER-GDEM ver1 SRTM Ver4.1 and GEODATA DEM-9 s Ver3 digital elevation models over Australia. Aust J Earth Sci **2010,** 57:337–347.

34. Pakoksung, K.; Takagi, M., Digital elevation models on accuracy validation and bias correction in vertical. Model. Earth Syst. Environ **2016**, 2(11) 1-13.DOI 10.1007/s40808-015-0069-3.
35. Graham, A.; Coops, N.C.; Wilcox, M.; Plowright, A. Evaluation of Ground Surface Models Derived from Unmanned Aerial Systems with Digital Aerial Photogrammetry in a Disturbed Conifer Forest. Remote Sens. **2019**, 11(84), 1-19. doi:10.3390/rs11010084.
36. Van Zyl, J.J. The shuttle radar topography mission (SRTM): A breakthrough in remote sensing of topography, Acta Astronautica **2001**, 48, 559–565.
37. Rabus, B.; Eineder, M.; Roth, A.M.; Bamler, R. The shuttle radar topography mission-a new class of digital elevation models acquired by space borne radar, J. Photogramm. Rem. Sens. **2004,** 57, 241–262.
38. Lemoine F. G.; Kenyon, S.C., Factor, J.K., Trimmer, R.G.; Pavlis, N.K.; Chinn, D.S.; Cox, C.M.; Klosko, S.M.; Luthcke, S.B.; Torrence, M.H.; Wang, Y.M.; Williamson; R.G.; Pavlis, E.C.; Rapp, R.H.; Olson, T.R. The Development of the Joint NASA GSFC and the National Imagery and Mapping Agency (NIMA) Geopotential Model EGM96n **1998,** NASA Technical Paper NASA/TP1998206 861, Goddard Space Flight Center, Greenbelt, Maryland.
39. Wessel, B., Huber, M., Wohlfart, C., Marschalk, U., Kosmann, D., Roth, A. Accuracy Assessment of the Global TanDEM-X Digital Elevation Model with GPS Data. ISPRS Journal of Photogrammetry and Remote Sensing, **2018,** 139 (l), 171-182.
40. Trimble. TrimbleInpho DTMaster Version 7.0 software (Licensed),**2015**, www.inpho.de.
41. Elkhrachy, I. Vertical accuracy assessment for SRTM and ASTER Digital Elevation Models: A case study of Najran city, Saudi Arabia. Ain Shams Engineering Journal **2018**, 9, 1807–1817.
42. Pavlis, N.K.; Holmes, S.A.; Kenyon, S.C.; Factor, J.K. The development and evaluation of Gravitational Model 2008 (EGM2008). Journal of Geophysical Research 2012, 117, 1-138. doi:10.1029/2011JB008916
43. Hipkin, R.G. Ellipsoidal geoid computation. J. Geodesy **2004**; 78:167-179.
44. Alamdari, M.N.; Emadi, S.R.; Moghtased-Azar, K. The ellipsoidal correction to the Stokes kernel for precise geoid determination, J Geod **2006**, 80: 675–689.
45. Hipkin, R.; Haines, K.; Beggan, C.; Bingley, R.; Hernandez, F.; Holt, J.; Baker, T. The geoid EDIN2000 and mean sea surface topography around the British Isles, Geophys.J.Int. **2004**, 157, 565–577.
46. Rexer, M., Hirt, C. Comparison of free high-resolution digital elevation datasets ASTER GDEM2, SRTM v2.1/v4.1. and validation against accurate heights from the Australian National Gravity Database. Australian Journal of Earth Sciences **2014**. 1-15. doi: 10.1080/08120099.2014.884983.
47. Ghandehari, M.; Buttenfield; B. P.; Carson,J.Q.F. Comparing the accuracy of estimated terrain elevations across spatial resolution, International Journal of Remote Sensing **2019,** 40:13, 5025-5049, DOI: 10.1080/01431161.2019.1577581.
48. American Society of Photogrammetric and Remote sensing (ASPRS), Accuracy standards for digital geospatial data, Photogrammetric Engineering and Remote Sensing **2013**; 79(12):1073–1085.
49. American Society of Photogrammetric and Remote sensing (ASPRS), ASPRS Positional Accuracy Standards for Digital Geospatial Data, November 2014, Photogrammetric Engineering and Remote Sensing **2015,** 81(3) 53 "http://www.asprs.org/"http://www.asprs.org/.
50. Hein, A. Processing of SAR data: fundamentals signal processing, interferometry, Springer-Verlag Berlin Heidelberg GmbH, Berlin, Germany, **2014**, pp291.
51. Rexer, M., Hirt, C. Comparison of free high-resolution digital elevation datasets ASTER GDEM2, SRTM v2.1/v4.1. and validation against accurate heights from the Australian National Gravity Database. Australian Journal of Earth Sciences **2014**. 1-15. doi: 10.1080/08120099.2014.884983.
52. The American Society for Photogrammetry and Remote Sensing (ASPRS). ASPRS Accuracy standards for large-scale maps 1990, Photogrammetric Engineering and Remote Sensing 56: 1068–70
53. Ministry of Urban Development, Housing and Construction. Urban Legal Cadastre Standard No. 03/2015, 2015, Technical report, Addis Ababa, Ethiopia.
54. Tachikawa, T.; Kaku, M.; Iwasaki, A.; Gesch, D.; Oimoen, M.; Zhang, Z.; Danielson, J.; Krieger, T.; Curtis, B.; Haase, J. ASTER Global Digital Elevation Model Version 2-Summary of Validation Results, **2011**. Retrieved on 16 March 2018. https://ssl.jspacesystems.or.jp/ ersdac/GDEM/ver2Validation/ Summary_ GDEM2_ validation_report_final.pdf.
55. Kolecka, N.; Kozak, J. Assessment of the Accuracy of SRTM C- and X-Band High Mountain Elevation Data: a Case Study of the Polish Tatra Mountains. Pure and Applied Geophysics, **2014,** 171(6), 897- 912.

56. Gdulová, K., Marešová, J., Moudrý, V. Accuracy assessment of the global TanDEM-X digital elevation model in a mountain environment. Remote Sensing of Environment **2020.** 241, 111724.
57. Wessel, B.; Gruber, A.; Huber, A.; Breunig, M.; Wagenbrenner, S.; Wendleder, A.; Roth, A., Validation of the absolute height accuracy of TanDEM-X DEM for moderate terrain. IGARSS IEEE, **2014**, 3394-3397. 58. Erasmi, S.; Rosenbauer, R.; Buchbach, R.; Busche, T.; Rutishauser, S. Evaluating the Quality and Accuracy of TanDEM-X Digital Elevation Models at Archaeological Sites in the Cilician Plain, Turkey, Remote Sensing **2014**,6 (10), 9475–9493.

Appendix I

Table 2. Common vertical accuracy classes for DEM points in non-vegetated and vegetated terrain (ASPRS, 2015).

Vertical accuracy class	RMSEz Non-Vegetated (cm)	Non-Vegetated Vertical Accuracy (NVA) (cm)	Vegetated Vertical Accuracy (VVA) at 95% (cm)	Equivalent class 1 contour interval per ASPRS 1990 (cm)	Equivalent class 2 contour interval per ASPRS 1990 (cm)
1 cm	1.0	2.0	3.0	3.0	1.5
2.5 cm	2.5	4.9	7.5	7.5	3.8
5 cm	5.0	9.8	15.0	15.0	7.5
10 cm	10.0	19.6	30.0	30.0	15.0
15 cm	15.0	29.4	45.0	45.0	22.5
20 cm	20.0	39.2	60.0	60.0	30.0
33.3 cm	33.3	65.3	99.9	99.9	50.0
66.7 cm	66.7	130.7	200.1	200.1	100.1
100 cm	100.0	196.0	300.0	300.0	150.0
333.3 cm	333.3	653.3	999.9	999.9	500.0